Riparian buffers act as microclimatic refugia in oil palm landscapes

Joseph Williamson[a*] 0000-0003-4916-5386
Eleanor M. Slade[b] 0000-0002-6108-1196
Sarah H. Luke[c,d] 0000-0002-8335-5960
Tom Swinfield[e] 0000-0001-9354-5090
Arthur Y. C. Chung[f] 0000-0002-9529-4114
David A. Coomes[e] 0000-0002-8261-2582
Herry Heroin[g]
Tommaso Jucker[h] 0000-0002-0751-6312
Owen T. Lewis[i] 0000-0001-7935-6111
Charles S. Vairappan[g] 0000-0001-7453-1718
Stephen J. Rossiter[a*] 0000-0002-3881-4515
Matthew J. Struebig[c] 0000-0003-2058-8502
[*]corresponding authors joseph.williamson@qmul.ac.uk, s.j.rossiter@qmul.ac.uk

[a]School of Biological and Chemical Sciences, Queen Mary University of London, Mile End Road, London, E14NS, UK

[b]Asian School of the Environment, Nanyang Technological University, 50 Nanyang Avenue, Singapore City, 639798, Singapore

[c]Durrell Institute of Conservation and Ecology (DICE), School of Anthropology and Conservation, University of Kent, Canterbury, UK

[d]Department of Zoology, University of Cambridge, Downing Street, Cambridge, CB2 3EJ, UK

[e]Department of Plant Sciences, University of Cambridge Conservation Research Institute, Downing Street, Cambridge, CB2 3EA, UK

[f]Forest Research Centre, Sabah Forestry Department, P.O. Box 1407, 90715 Sandakan, Sabah, Malaysia

[g]Institute for Tropical Biology and Conservation, Universiti Malaysia Sabah, Kota Kinabalu 88440, Sabah, Malaysia

[h]School of Biological Sciences, University of Bristol, 24 Tyndall Ave, Bristol, BS8 1TQ, UK

[i]Department of Zoology, University of Oxford, South Parks Road, Oxford, OX1 3PS, UK

Abstract

1. There is growing interest in the ecological value of set-aside habitats around rivers in tropical agriculture. These riparian buffers typically comprise forest or other non-production habitat, and are established to maintain water quality and hydrological processes, whilst also supporting biodiversity, ecosystem function and landscape connectivity.
2. We investigated the capacity for riparian buffers to act as microclimatic refugia by combining field-based measurements of temperature, humidity, and dung beetle communities with remotely-sensed data from LiDAR across an oil palm dominated landscape in Borneo.
3. Riparian buffers offer a cool and humid habitat relative to surrounding oil palm plantations, with wider buffers characterised by conditions comparable to riparian sites in continuous logged forest.
4. High vegetation quality and topographic sheltering were strongly associated with cooler and more humid microclimates in riparian habitats across the landscape. Variance in beetle diversity was also predicted by both proximity-to-edge and microclimatic conditions within the buffer, suggesting that narrow buffers amplify the negative impacts that high temperatures have on biodiversity.
5. *Synthesis and applications.* Widely-legislated riparian buffer widths of 20-30 m each side of a river may provide drier and less humid microclimatic conditions than continuous forest. Adopting wider buffers and maintaining high vegetation quality will ensure set-asides established for hydrological reasons bring co-benefits for terrestrial biodiversity, both now, and in the face of anthropogenic climate change.

Keywords

riparian reserve biodiversity tropical forest Borneo habitat fragmentation agriculture

1. Introduction

Microclimate determines how organisms interact with their surroundings, from development and physiology, to behaviour, ecology, function and distribution (Jucker et al., 2020). The need to understand how microclimate varies across land-use mosaics is acute in the wet tropics, where high biodiversity is threatened by the combined impacts of rapid land-use change and climatic warming (Travis, 2003). Fine-scale microclimate is shaped by multiple environmental factors, including solar radiation, wind, topography and vegetation structure (Helmuth, 2009). As such, microclimatic gradients are particularly pronounced across tropical agriculture-forest mosaics, where vegetation structure can vary dramatically (Blonder et al., 2018; Jucker et al., 2018). Degraded forests have higher temperatures and lower humidities than undisturbed forests (Hardwick et al., 2015), although both are cooler than farmland (Hardwick et al., 2015; Silvério et al., 2015; Meijide et al., 2018).

Riparian buffers, or riparian reserves, are areas of non-production habitat (often forest) retained around rivers in agricultural landscapes, primarily as a means of protecting water quality by reducing run-off (Tabacchi et al. 2000). In many tropical nations, riparian buffers of a designated width are required by law, often based on the size of the river in question (Luke et al., 2019a). In addition, policies on riparian buffer width have been adopted by groups such as the Roundtable on Sustainable Palm Oil (RSPO) as part of their certification criteria for mitigating the detrimental impacts of oil palm development on the environment and local communities (Luke et al., 2019a). In addition to their primary role in protecting water quality, riparian buffers provide a range of other ecosystem services, such as carbon storage (Mitchell et al., 2018), flood protection (Tabacchi et al., 2000) and subsidising water courses with terrestrially-derived organic matter (Allan, 2004). Buffers can also provide co-benefits for a variety of terrestrial (Barlow et al., 2010; Keir et al., 2015; Zimbres et al., 2017) and aquatic taxa (Cunha & Juen, 2017; Giam et al., 2015). There are also examples of these habitat remnants serving as corridors between other forest areas, promoting connectivity for various taxa (Gray et al., 2019; Keuroghlian & Eaton, 2008).

In common with all habitat fragments, the efficacy of riparian buffers for safeguarding biodiversity and promoting connectivity will depend on habitat area and quality, the level of contrast with the surrounding matrix, and the biology of the taxa in question (Lees & Peres, 2008). In general, the attributes of riparian buffers that support terrestrial biodiversity remain poorly understood. Recent studies have demonstrated the role of buffer width for birds (Lees & Peres, 2008; Keir et al., 2015; Mitchell et al., 2018), mammals (Zimbres et al., 2017) and dung beetles (Barlow et al., 2010; Gray et al., 2017), with several subsequently linking observed biodiversity patterns to habitat quality (Lees & Peres, 2008; Mitchell et al., 2018). However, studies investigating riparian buffer microclimates and the features that shape them are scarce (e.g. Nagy et al., 2015).

Insights into the effects of microclimate on tropical biodiversity are often limited by issues of scale and accuracy (Jucker et al., 2018; Schulze et al., 2001), with most studies relying on coarse-resolution mapping databases such as WorldClim (Fick & Hijmans, 2017). Advances in technologies such as Light Detection And Ranging (LiDAR) make it possible to map landscapes and vegetation with unprecedented levels of accuracy and precision (Zellweger et al., 2019), allowing studies to better quantify and link physical habitat structure to microclimate (Lefsky et al., 2002). The decreasing costs of microclimatic dataloggers have also catalysed an

increase in research investigating fine-scale microclimatic conditions (e.g. Hardwick et al., 2015; Law et al. 2019).

Here we combine information from airborne LiDAR with field-based microclimatic measurements to investigate the efficacy of forested riparian buffers of different widths and habitat composition for providing microrefugia within oil palm plantations. We deployed dataloggers across three riparian habitats: oil palm, riparian buffers, and continuous logged-forest, in Sabah, Malaysian Borneo. First, we examine if riparian buffers in otherwise microclimatically-extreme plantations maintain conditions similar to those found in continuous riparian forest. We then demonstrate how vegetation conditions and topography shape the microclimate within riparian buffers, and across human-modified landscapes as a whole, before evaluating how edge effects influence buffer microclimate and the implications this has for policy pertaining to buffer width. Finally, to assess the capacity of tropical riparian buffers to act as microrefugia for a key invertebrate indicator group (*Scarabaeinae*), we couple the microclimatic data with dung beetle community data across the modified landscape.

2. Material and Methods

2.1 Study Site

Fieldwork was conducted in and around the Stability of Altered Forest Ecosystems project (www.safeproject.net; 4°81'N 117°25'E - 4°43'N 117°64'E, plot elevation ranged from 125-450 m a.s.l) in Sabah, Malaysia (Northern Borneo, Figure 1A). This region is characterised by a tropical climate, with annual rainfall ~2,700 mm and a mean annual temperature of 26.7°C (Walsh & Newbery, 1999), although a recent study shows the region has become hotter and drier in recent years (Chapman et al., 2020). The area was formerly continuous lowland dipterocarp forest with much of the remaining forest having been selectively logged in the 1970s and 2000s, and subsequently salvage logged in 2013 and 2015 in preparation for oil palm (Struebig et al., 2013). At the time of fieldwork, this forest was highly fragmented, bounded to the north by continuous forest, and surrounded by oil palm plantations (planted 8-12 years previously) elsewhere (Figure 1).

Between December 2016 and May 2018, we deployed dataloggers (EasyLog USB, Lascar Electronics) in 300 locations across 60 transects (5 dataloggers per transect) on 20 rivers (3 transects per river) in the landscape: in oil palm plantations (OP: *n=2* rivers, 6 transects), riparian forest buffers within oil palm plantations (RB: *n=16* rivers, 48 transects) and continuous logged forest (CF: *n=2* rivers, 6 transects). Distances between adjacent transects on a river were 342-591 m, with rivers varying from 0.5 - 48 km apart (median 18km). In oil palm and continuous forest, dataloggers were deployed in transects perpendicular to the riverbank at distances of 5 m, 15 m, 25 m, 35 m and 45 m. In riparian buffer transects, dataloggers were deployed at 5 m and 15 m from the riverbank and at ~5 m from the buffer-oil-palm edge, and at 5 m and 25 m into the oil palm Figure 1D). A range of buffer widths (0-324 m) were investigated to investigate the effect of proximity-to-edge on microclimate. All units were suspended at 3 m above the ground with a polystyrene plate rain-cover and left to record temperature (*T,* °C) and relative humidity (RH, %) for 3-7 weeks at intervals of 30 minutes.

2.2 Microclimate Data

Datalogger data were collated to calculate maximum (T_{max}) and mean (T_{mean}) daily temperatures for each sampling day. RH was used to calculate vapour pressure deficit (VPD, hPa) - the difference in the partial pressure of water vapour in the air compared with saturated air at a given temperature (*T*):

$$VPD = \frac{100 - RH}{100} e_s, \text{ where } e_s = 6.112e^{\frac{17.67T}{T+243.5}}$$

VPD represents the evaporative demand of the air, pulling water up through the soil-root-stem-leaf continuum. Thus, it is a critical determinant of plant ecology, strongly influencing potential evapotranspiration and the ability of plants to supply their leaves with sufficient water during the driest parts of the day, and thereby regulating seedling growth and mortality (Williams et al., 2013). Maximum (VPD_{max}) and mean (VPD_{mean}) daily VPD were generated for each sampling day.

2.3 Vegetation Quality, Topography and Distance from Buffer-Oil-Palm Edge

To understand how vegetation quality and topography influence microclimate in riparian habitats we used airborne LiDAR data collected over part of the landscape (see Jucker et al., 2018). For the 35 transects coinciding with the 2014 LiDAR information we extracted a set of

vegetation and topographic metrics from the canopy height, digital terrain and plant area index model rasters, using a 12.5 m radius extraction. LiDAR-derived metrics were mean plant area index (PAI, log-transformed), maximum canopy height (H_{max}), topographic position index (TPI), elevation, aspect and slope. PAI was calculated empirically from the raw LiDAR data as an integrated measure of canopy density (m^2 m^{-2}; Holst et al., 2004). H_{max} (m) was calculated as the maximum canopy height value (after ground-normalising the LiDAR point cloud) within 12.5 m of the logger. Four topographic covariates were calculated using the *terrain* function in the *raster* package (Hijmans, 2016) in R 3.6.1 (R Development Core Team, 2008): elevation in (m.a.s.l.), slope (in degrees), aspect (in radians) and TPI - the difference between the elevation of a point and the average of its surroundings (positive values on ridges and negative values in depressions). Aspect was sinewave transformed so that east- and west-facing slopes had positive and negative values respectively. Our metrics were selected *a priori* following Jucker et al. (2018), who chose them due to their weak correlation (Supplementary Figure 1), and known effects on microclimate in tropical rainforests. The distance into riparian buffers from the buffer-oil-palm edge was measured on the canopy height model in QGIS 3.10.4 using the ruler tool (QGIS Development Team, 2020), as a proxy for examining the effects of manipulating buffer width on microclimate. For dataloggers associated with riparian buffers outside the LiDAR area (n=22 transects), distances from the buffer-oil-palm edge were measured manually for buffer edge sites. River width was subtracted from total buffer width (as calculated from Google Earth imagery) and halved to give an estimate of buffer width for each transect. Distance from river was then subtracted from buffer width to give estimates of distance from edge for buffer core sites.

2.4 Dung Beetle Diversity Sampling

To understand how microclimate impacts the efficacy of riparian buffers as a means of supporting biodiversity, we carried out two dung beetle (*Scarabaeinae*) sampling campaigns, in January 2015 and from September 2017 to March 2018. The climate in our study landscape is relatively aseasonal (Walsh & Newbery, 1999), although sampling dates broadly correspond to the marginally wetter season (Marsh & Greer, 1992), where dung beetle activity is highest. Dung beetles are a useful indicator group due to their sensitivity to disturbance, high diversity, well-established taxonomy, ease of sampling, and importance for a range of ecosystem functions (Nichols & Gardner, 2013). Like most tropical ectotherms, dung beetles are thought to be operating close to their thermal maxima, putting them at a greater risk of extinction due to climatic shifts (Deutsch et al., 2008). Dung beetle assemblages were sampled using human-dung-baited pitfall traps (following Slade et al., 2011). For each datalogger transect in a buffer (n=48), one trap was deployed for two trapping nights ~10 m from the river. The minimum distance between transects with traps was 381 m. Beetles were collected into 90% ethanol and identified to species or morpho-species using reference collections housed at the Universiti Malaysia Sabah.

2.5 Statistical Analyses

2.5.1 Riparian Buffers as Microclimatic Refugia

To examine whether riparian buffers and plantations maintain microclimatic conditions similar to those found in continuous riparian forest, we ran a mixed-effects model of each of our four microclimatic response variables (T_{max}, T_{mean}, VPD_{max} and VPD_{mean}) against a fixed effect of

four habitat types: continuous forest, riparian buffer core (buffer interior >10 m from the buffer-oil-palm edge, hereafter referred to as buffer core), riparian buffer edge (buffer interior ≤10 m of the buffer-oil-palm edge, hereafter referred to as buffer edge) and oil palm. Sampling transect was fitted as a random effect, and models were run in the *lme4* package in R (Bates et al., 2015) with a Gaussian error distribution. Habitat-type models were compared against the null model (only containing the random-effect) by comparing AIC, where a difference of -4 supports one nested model over another (Bolker, 2008).

2.5.2 Effects of Vegetation Quality and Topography on Microclimate

To analyse the effects of vegetation quality and topography on microclimate, we took a subset of our data from 36 transects that coincided with LiDAR information. We defined separate maximal linear mixed-effects models for each of our four microclimatic response variables (T_{max}, T_{mean}, VPD_{max} and VPD_{mean}) with all of our seven explanatory variables (PAI, H_{max}, TPI, elevation, aspect, slope and habitat) fitted as fixed effects, and with one interaction term (H_{max} : aspect) following Jucker et al. (2018), with sampling transect as a random effect and a Gaussian error distribution. By sequential removal of terms, every possible subset of each maximal model was generated (159 for each response variable) and ranked by AIC weight in the *bbmle* package in R (Bolker & R Development Core Team, 2017). Models were then subsetted to retain the fewest possible models that cumulatively accounted for 0.95 or more of the total AIC weight. The AIC weighted proportion of explanatory variable retention in the final models is reported.

2.5.3 Edge Effects on Buffer Microclimate

We examined the impact of edge effects on microclimatic conditions using distance from buffer-oil-palm edge. We analysed a subset of the full data that only included dataloggers deployed within riparian buffers (both buffer edge and core habitat types). Similar to the aforementioned habitat type analyses, each of the four microclimatic response variables (T_{max}, T_{mean}, VPD_{max} and VPD_{mean}) were entered into mixed-effects models with distance into buffer from edge fitted as a fixed effect, sampling transect as a random effect and a Gaussian error distribution. Models were then compared to respective null models using AIC.

2.5.4 Buffer Microclimate Impacts on Dung Beetle Diversity

To analyse how riparian buffer microclimate impacts biodiversity, we matched our dung beetle assemblage samples to buffer core dataloggers. Microclimate data from sites 5 m from the river were used, unless data were only available from points 15 m from the river. Dung beetle diversity, calculated as Shannon diversity in the *vegan* package in R (Oksanen et al., 2010), was fitted as the response variable in four maximal linear models (for each of T_{max}, T_{mean}, VPD_{max} and VPD_{mean}) with a Gaussian error distribution. Each maximal model had distance from buffer edge (log-transformed), the microclimate variable of interest and an interaction term between the two, as explanatory variables. For each microclimatic explanatory variable, all possible combinations of explanatory variables were compared to the maximal model using dAIC. Similar analyses were conducted for species richness (see Supplementary Methods).

3. Results

Of the 300 dataloggers deployed in riparian transects, 198 were recovered fully-functioning, resulting in 5,438 days of microclimatic recordings. Of the 198 units, 110 were recovered within the LiDAR area, whilst 79 were located in riparian buffer core or edge and had width data available (Supplementary Table 1). All microclimatic variables (T_{max}, T_{mean}, VPD_{max} and VPD_{mean}) were strongly correlated (Pearson's $r > 0.6$, Supplementary Table 2).

3.1 Riparian Buffers as Microclimatic Refugia

We found strong support for the impact of habitat type on T_{max}, T_{mean}, VPD_{max} and VPD_{mean}, when compared to a null-model (fitted with only a random effect of transect) (dAICs : T_{max} = -53.5; T_{mean}= -100.9; VPD_{max} = -40.8; VPD_{mean}. = -91.6). All microclimatic variables showed similar responses to habitat type (Figure 2), with the coolest and wettest conditions in continuous riparian forest (Table 1). Buffer core microclimates were intermediate between continuous forest and the hotter and drier oil palm, whereas buffer edge sites had maximum daily values greater than those of oil palm, and mean daily values similar to, or slightly less than, those of oil palm (Table 1).

3.2 Effects of Vegetation Quality and Topography on Microclimate

Data from units within the LiDAR area were used to model the impacts of vegetation quality and topography on microclimate across the study landscape, encompassing the riparian buffers and other habitat types. Of the best-fitting models that cumulatively accounted for an AIC weight of 0.95, the lowest-weighted models were still strongly supported when compared to the null model for each microclimatic variable (dAIC : T_{max} = -45.89; T_{mean}= -113.05; VPD_{max} = -21.21; VPD_{mean}. = -72.29). In these best-fitting models, variables relating to both vegetation quality and topography were retained. Specifically, PAI was a strong negative predictor of all four microclimatic variables and H_{max} was a negative predictor of T_{mean} (Figure 3, Table 2). TPI was a strong positive predictor of all four microclimatic variables (Figure 3). Elevation was a weak predictor of T_{max} and T_{mean}, with an increase of 100 m elevation resulting in a mean drop of 0.27°C (Table 2). Aspect was a weak predictor of T_{mean} and VPD_{mean}, with east-facing slopes being hotter and drier than west-facing slopes (Table 2). Slope and the interaction term between H_{max} and aspect were not frequently retained in best-fitting models (Table 2). Habitat type, the only non-LiDAR derived variable, was retained in the best-fitting models for T_{max}, T_{mean} and VPD_{mean} (Table 2).

3.3 Edge Effects on Buffer Microclimate

Linear mixed-effects models of distance into the buffer from the buffer-oil-palm edge (log-transformed) were strongly supported when compared to the null-models (dAIC : T_{max} = -15.65; T_{mean}= -20.75; VPD_{max} = -10.58; VPD_{mean}. = -17.96). All microclimatic response variables had negative relationships with distance from edge (T_{max} = -1.40 ± 0.31, T_{mean}= -0.24 ± 0.05, VPD_{max} = -3.39 ± 0.93, VPD_{mean}. = -0.58 ± 0.12) (Figure 4). At approximately 80-120 m from the edge, predicted curves for each microclimatic variable become relatively flat, and for T_{max}, T_{mean} and VPD_{mean} begin to be comparable to those of continuous riparian forest values, (Figure 4). All models had Cook's distances < 0.5 (Supplementary Figure 2).

3.4 Buffer Microclimate Impacts on Dung Beetle Diversity

Of the 48 transects associated with riparian buffers, 31 had functioning dataloggers in the buffer core, with associated data on both dung beetle diversity and distance from edge into buffer. Dung beetle diversity was driven by an interaction between distance from buffer edge and both T_{max} and T_{mean} (Table 3). As distance from the edge decreased, the relationship between temperature (T_{max} and T_{mean}) and dung beetle diversity became more negative, whereas at 80 m it is relatively flat (Figure 5). Responses for the interaction between VPD and distance from edge were similar to those of temperature but with lower AIC weight, particularly for VPD_{mean} (Table 3). Further, lower dung beetle diversity was associated with higher T_{mean}, VPD_{max} and VPD_{mean}, (Tables 3 and 4). Note, the VPD_{max} model lacking an interaction term failed our leverage tests and must be regarded with caution (Supplementary Figure 3). Species richness analyses showed similar responses to Shannon diversity (see Supplementary Results).

4. Discussion

Our results demonstrate the capacity of riparian buffers to provide microclimatic refugia in human-modified tropical landscapes. All four measures of temperature and vapour pressure deficit (T_{max}, T_{mean}, VPD_{max} and VPD_{mean}) were lower in the core area of riparian buffers than in the surrounding oil palm, although these values were still higher than those in continuous riparian forest. We reveal that buffer edge effects mediate microclimate, with the interior of the buffer being substantially cooler and more humid than edges and plantation. We subsequently demonstrate the key roles that greater vegetation complexity and topographic sheltering play in increasing the microclimatic buffering capacity of these set-asides. Finally, we elucidate the link between buffer width and microclimate, and dung beetle communities, revealing that proximity-to-edge and temperature can synergistically decrease local diversity.

Consistent with our results, Nagy et al. (2015) found that microclimates in riparian buffer cores in the southern Amazon were comparable to those of continuous riparian forests. Cooler and wetter conditions here were more strongly associated with wide buffers, particularly those 80 m or more in width (Table 5). Although our buffer core sites were generally cooler than oil palm, edge habitat was characterised by more extreme conditions than adjacent plantation. Oil palm is a perennial crop with a peak yield occurring at an age of 9-18 years (Alam et al., 2015), with older plantations forming tall canopies with cooler microclimates (Luskin & Potts, 2011). We postulate that high T_{max} and VPD_{max} in buffer edges is due to gaps in vegetation associated with riparian buffer edges (JW personal observation). Such gaps are dominated by bare ground, grasses or low-lying vines, and may be due to clearing and spillover of herbicides from the plantation. The gaps could also elevate T and VPD for short periods of the day. The temperature and humidity extremes in buffer edges are consistent with well-documented microclimatic changes seen in other edge habitats, which are typically attributed to increased solar radiation and wind (see Williams-Linera, 1990).

We reveal the link between several vegetation and topographic features, and microclimate, across a human-modified tropical landscape. In particular, PAI, a measure of vegetation quality, had a strong influence on microclimate. Increased PAI is associated with more complex vegetation (Holst et al., 2004), causing decreased wind and light exposure to give cool, humid conditions (Hardwick et al., 2015). H_{max} (maximum canopy height) was also strongly associated with T_{mean}, a relationship driven by increased shading by tall trees (Jucker et al., 2018). Like other edge habitats, riparian buffers are characterized by factors impacting vegetation structure, with reduced seedling abundance, tree basal area, canopy height and woody plant diversity compared with continuous riparian forest (Lees & Peres, 2007, Keir et al., 2015, Nagy et al., 2015). Topography was also a key predictor of our microclimatic variables, with TPI having strong positive correlations with temperature and VPD. Such results are indicative of the relative exposure of ridges (high TPI) and depressions (low TPI) to light and wind (Dobrowski, 2011). Aspect had a small positive effect on T_{mean} and VPD_{mean}, where east-facing slopes tended to be hotter and drier, likely due to daily solar radiation and wind patterns in the region (Smith, 1977). Elevation negatively predicted T_{max} and T_{mean}, with a 100 m increase resulting in a mean drop of 0.27°C, a lower impact than we might expect given the literature (Jucker et al., 2018) and likely due to a limited range of elevations in our study. Our results highlight the importance of understanding how heterogeneous vegetation and topography must be taken into account when defining the extent of riparian buffers in environmental policies, as well as predicting landscape- or regional-level diversity responses under climate change scenarios (Elsen et al., 2020).

The cooler, wetter microclimate of riparian buffers described here makes them likely refugia for biodiversity in a hostile agricultural matrix. Indeed, our results indicate that microclimate in buffers may be important for driving diversity patterns in dung beetles, a key invertebrate indicator group. We found that at 80 m from the edge, the response of beetle diversity to temperature was negligible. However, as proximity to the buffer-oil-palm edge increased, the negative effects of temperature on diversity were amplified, with beetle communities in 20m buffers acutely sensitive to higher temperatures. Previous research within the same landscape found riparian buffers support higher diversity than surrounding oil palm plantations, with dung beetle assemblages more similar to those of continuous riparian forests than oil palm (Gray et al., 2014). Further, Gray et al. (2016) demonstrated little spillover of dung beetle species within riparian buffers into the surrounding oil palm plantations. Combined with our findings, this suggests that riparian buffers may act as microrefugia for forest invertebrates. Note that the effects of microclimatic variables shown here could be correlative rather than causative. As we have demonstrated, topography and vegetation complexity can also drive microclimatic conditions, and it is difficult to disentangle these effects. This does not however, change the take-home message of the results - to maximise co-benefits for terrestrial biodiversity in riparian buffers, simply regulating buffer width alone is likely to be insufficient if this does not preserve the vegetation and topographic features that are needed to help maintain a buffered microclimate.

In addition to microclimate, we also found that distance from edge was associated with higher local diversity, supporting a pool of literature demonstrating the positive impact of increased buffer width on terrestrial biodiversity (Gray et al., 2017; Keir et al., 2015; Zimbres et al., 2018). Intriguingly, the widths recommended by these previous studies to retain terrestrial biodiversity (80 m for dung beetles and forest-specialising birds; Gray et al., 2017; Mitchell et al., 2018) are in the region where some of our proximity-to-edge microclimatic response curves intersect with the 95% confidence interval for continuous forest and where edge effects generally tail off in many systems (e.g. Didham & Lawton 1999; Laurence et al., 2002). The consequences of edge effects for biodiversity may be more pronounced in tropical landscapes with sparse open habitat where species have not experienced long-term selection pressures for avoiding edges (Betts et al., 2020). Ideally, edge effects would be investigated in the same set of models as vegetation quality, however, due to strong correlations between proximity-to-edge and our LiDAR-derived variables, this was not possible.

4.1 Policy Implications

Our results are important to riparian buffer policies in human-modified tropical landscapes, supporting suggestions that mandatory riparian buffer widths in the tropics should be wider than they currently are, that more attention should be given to buffer habitat quality (Luke et al., 2019a), and that topography should also be considered when planning networks of buffers across landscapes. We show that buffers begin to reach microclimatic conditions comparable to those of continuous riparian forest at approximately 80 m and above, on each side of the river, a width previously suggested as adequate for maintaining representative levels of species diversity (Gray et al., 2017, Mitchell et al., 2018). At this buffer width, the negative impacts of temperature on biodiversity are far less pronounced than at 20 m, the width typically required by law in Sabah, Malaysia. These recommendations are emphasised by the finding that buffer edges, and thus narrow buffers (<10 m), may be more microclimatically extreme than no buffer at all. In addition, many tropical countries do not consider vegetation complexity in riparian management policies (Luke et al., 2019a), but doing so could help contribute to improved microclimate conditions and long-term sustainability of waterways in agricultural areas. We therefore advocate efforts to extend buffer widths, prevent further degradation and restore

412 riparian buffers (Luke et al., 2019b). In addition, by determining the vegetation and topographic
413 features that drive microclimate in tropical riparian buffers, we hope to inform the future
414 planning of buffer locations and networks. Taken together, our results suggest that
415 safeguarding riparian buffer microclimate may help to limit the local extinction of species by
416 providing microrefugia. This finding is likely to become increasingly important in the face of
417 anthropogenic climate change (Hampe & Jump, 2011), particularly if demand for agricultural
418 land near water-bodies increases with drier climates.

Acknowledgements

This work was funded by the Natural Environmental Research Council (NERC) through the Human Modified Tropical Forests programme (NE/K016261/1; NE/K016377/1), as well as the Newton--Ungku Omar Fund via the British Council and Malaysian Industry -Government Group for High Technology (216433953). NERC also funded the PhD studentship for JW (NE/L002485/1) and research fellowship of TJ (NE/S01537X/1). We are grateful to the Sabah Biodiversity Council for permission to conduct the fieldwork (SL: JKM/MBS.1000-2/2JLD.5(13); JW: JKM/MBS.1000-2/2JLD.7(83); EMS: JKM/MBS.1000-2/2(381)), Jonathan Parrett for help with dung beetle identification, and the South East Asian Rainforest Research Programme staff, who made this work possible: Unding Jami, Johnny Larenus, Amir, Anis, David, Didy, Dino, Joanni, Kiki, Loly, Mudin, Noy and Zul.

The authors have no conflicts of interest to declare.

Author Contributions

MJS and EMS conceived the initial project and research design; they and DAC, OTL, SJR and CSV secured funding; SHL, EMS and HH undertook the fieldwork; TS, TJ and DAC contributed LiDAR data; JW and EMS identified the dung beetles with support from AYCC; JW led the analysis and writing of the manuscript with input from the rest of the team.

Data Accessibility

Microclimate data are available at 10.5281/zenodo.4000206.
LiDAR data are available at: https://dx.doi.org/10.5285/edf7a41f4c4a40b8946c21ab1cab5d47
http://dx.doi.org/10.5285/1a072df93a19434e85b4fff7fabfdafa
http://dx.doi.org/10.5285/a88dca766a6f4059bf60a866258f4903
http://dx.doi.org/10.5285/340711b723124764bd42f39c4465d728
http://dx.doi.org/10.5285/2ffddce56f01468b888b01942eba75dc
http://dx.doi.org/10.5285/eb49848446ef41dcad6c45658b8c644a
http://dx.doi.org/10.5285/4b30bf7c8f1243bcbc70c4816356a8d6
http://dx.doi.org/10.5285/ca81ecd6acd441ac89fc5b505a355102
http://dx.doi.org/10.5285/3f7d71a981d341708bcb4db1edbff62e.
Dung beetle data are available for 2015 and 2017/8 at https://doi.org/10.5281/zenodo.3906118 and https://doi.org/10.5281/zenodo.3906441.

References

Alam, A.F., Er, A.C. & Begum, H. (2015). Malaysian oil palm industry: prospect and problem. *Journal of Food, Agriculture & Environment*, *13*(2), 143-148.

Allan, J.D. (2004). Landscapes and riverscapes: the influence of land use on stream ecosystems. *Annual Review of Ecology, Evolution and Systematics*, *35*, 257-284.

Barlow, J., Louzada, J., Parry, L., Hernández, M. I. M., Hawes, J., Peres, C. A., … Gardner, T. A. (2010). Improving the design and management of forest strips in human-dominated tropical landscapes: A field test on Amazonian dung beetles. *Journal of Applied Ecology*, *47*, 779–788.

Bates, D., Maechler. M, Bolker, B., & Walker, S. (2015). Fitting Linear Mixed-Effects Models Using lme4. *Journal of Statistical Software*, *67*(1), 1-48.

Betts, M.G., Wolf, C., Pfeifer, M., Banks-Leite, C., Arroyo-Rodríguez, V., Ribeiro, D.B., ... Hadley, A.S. (2020). Extinction filters mediate the global effects of habitat fragmentation on animals. *Science*, *366*(6470), 1236-1239.

Bolker, B.M. (2008). E*cological models and data in R.* Princeton University Press, 210.

Bolker, B. & R Development Core Team (2017). bbmle: Tools for General Maximum Likelihood Estimation. R package version 1.0.20. https://cran.r-project.org/web/packages/bbmle/index.html.

Blonder, B., Both, S., Coomes, D.A., Elias, D., Jucker, T., Kvasnica, ... Svátek, M. (2018). Extreme and highly heterogeneous microclimates in selectively logged tropical forests. *Frontiers in Forests and Global Change*, *1*, 5.

Chapman, S., Syktus, J.I., Trancoso, R., Salazar, A., Thatcher, M.J., Watson, J.E., ... McAlpine, C.A. (2020). Compounding impact of deforestation on Borneo's climate during El Niño events. *Environmental Research Letters*. *15*, 084006.

Cunha, E. J., & Juen, L. (2017). Impacts of oil palm plantations on changes in environmental heterogeneity and Heteroptera (Gerromorpha and Nepomorpha) diversity. *Journal of Insect Conservation*, *21*, 111–119.

Deutsch, C.A., Tewksbury, J.J., Huey, R.B., Sheldon, K.S., Ghalambor, C.K., Haak, D.C. & Martin, P.R. (2008). Impacts of climate warming on terrestrial ectotherms across latitude. *Proceedings of the National Academy of Sciences*, *105*(18), 6668-6672.

Didham, R.K. & Lawton, J.H. (1999). Edge structure determines the magnitude of changes in microclimate and vegetation structure in tropical forest fragments. *Biotropica*, *31*(1), 17-30.

Dobrowski, S.Z. (2011). A climatic basis for microrefugia: the influence of terrain on climate. *Global change biology*, *17*(2), 1022-1035.

Elsen, P.R., Monahan, W.B. & Merenlender, A.M. (2020). Topography and human pressure in mountain ranges alter expected species responses to climate change. *Nature Communications*, *11*(1), 1-10.

Fick, S.E. & Hijmans, R.J. (2017). WorldClim 2: new 1-km spatial resolution climate surfaces for global land areas. *International Journal of Climatology*, *37*(12), 4302-4315.

Giam, X., Hadiaty, R. K., Tan, H. H., Parenti, L. R., Wowor, D., Sauri, S., & Wilcove, D. S. (2015). Mitigating the impact of oil-palm monoculture on freshwater fishes in Southeast Asia. *Conservation Biology*, *29*, 1357–1367.

Gray, C.L., Slade, E.M., Mann, D.J. & Lewis, O.T. (2014). Do riparian reserves support dung beetle biodiversity and ecosystem services in oil palm-dominated tropical landscapes?. *Ecology and Evolution*, *4*(7), 1049-1060.

503 Gray, C.L., Simmons, B.I., Fayle, T.M., Mann, D.J. & Slade, E.M. (2016). Are riparian forest
504 reserves sources of invertebrate biodiversity spillover and associated ecosystem
505 functions in oil palm landscapes?. *Biological Conservation*, *194*, 176-183.
506 Gray, C., Slade, E., Mann, D. & Lewis, O.T. (2017). Designing oil palm landscapes to retain
507 biodiversity using insights from a key ecological indicator group. *bioRxiv*, 204347.
508 Gray, R.E.J., Slade, E.M., Chung, A.Y. & Lewis, O.T. (2019). Movement of moths through
509 riparian reserves within oil palm plantations. *Frontiers in Forests and Global Change*,
510 *2*, 68.
511 Hampe, A. & Jump, A.S. (2011). Climate relicts: past, present, future. *Annual Review of*
512 *Ecology, Evolution, and Systematics*, *42*, 313-333.
513 Hardwick, S.R., Toumi, R., Pfeifer, M., Turner, E.C., Nilus, R. & Ewers, R.M. (2015). The
514 relationship between leaf area index and microclimate in tropical forest and oil palm
515 plantation: Forest disturbance drives changes in microclimate. *Agricultural and Forest*
516 *Meteorology*, *201*, 187-195.
517 Helmuth, B. (2009). From cells to coastlines: how can we use physiology to forecast the
518 impacts of climate change? *Journal of Experimental Biology*, *212*(6), 753-760.
519 Hijmans, R. J. (2016). raster: Geographic data analysis and modeling. R package version 2.5–
520 8. https://CRAN.R-project.org/package=raster.
521 Holst, T., Hauser, S., Kirchgäßner, A., Matzarakis, A., Mayer, H. & Schindler, D., 2004.
522 Measuring and modelling plant area index in beech stands. *International Journal of*
523 *Biometeorology*, *48*(4), 192-201.
524 Jucker, T., Hardwick, S.R., Both, S., Elias, D.M., Ewers, R.M., Milodowski, D.T., ... Coomes,
525 D.A. (2018). Canopy structure and topography jointly constrain the microclimate of
526 human-modified tropical landscapes. *Global change biology*, *24*(11), 5243-5258.
527 Jucker, T., Jackson, T.D., Zellweger, F., Swinfield, T., Gregory, N., Williamson, J., ...
528 Coomes., D.A. (2020). A research agenda for microclimate ecology in human-modified
529 tropical forests. *Frontiers in Forests and Global Change*, *2*, 92.
530 Keir, A. F., Pearson, R. G., & Congdon, R. A. (2015). Determinants of bird assemblage
531 composition in riparian vegetation on sugarcane farms in the Queensland wet tropics.
532 *Pacific Conservation Biology*, *21*, 60–73.
533 Keuroghlian, A. & Eaton, D.P. (2008). Importance of rare habitats and riparian zones in a
534 tropical forest fragment: preferential use by Tayassu pecari, a wide-ranging frugivore.
535 *Journal of Zoology*, *275*(3), 283-293.
536 Laurance W.F., Lovejoy T.E., Vasconcelos H.L., Bruna E.M., Didham R.K., Stouffer P.C., ...
537 Sampaio, E. (2002) Ecosystem decay of Amazonian forest fragments: a 22-year
538 investigation. *Conservation Biology*, *16*, 605–618.
539 Law, S.J., Bishop, T.R., Eggleton, P., Griffiths, H., Ashton, L. and Parr, C. (2020). Darker ants
540 dominate the canopy: Testing macroecological hypotheses for patterns in colour along
541 a microclimatic gradient. *Journal of Animal Ecology*, *89*(2), 347-359.
542 Lees, A.C. & Peres, C.A. (2008). Conservation value of remnant riparian forest corridors of
543 varying quality for Amazonian birds and mammals. *Conservation biology*, *22*(2), 439-
544 449.
545 Luke, S.H., Slade, E.M., Gray, C.L., Annammala, K.V., Drewer, J., Williamson, J., ... Struebig,
546 M.J. (2019a). Riparian buffers in tropical agriculture: Scientific support, effectiveness
547 and directions for policy. *Journal of Applied Ecology*. *56*, 85– 92.
548 Luke, S.H., Advento, A.D., Aryawan, A.A.K., Adhy, D.N., Ashton-Butt, A., Barclay, H., ...
549 Eycott, A.E. (2019b). Managing oil palm plantations more sustainably: large-scale
550 experiments within the Biodiversity and Ecosystem Function in Tropical Agriculture
551 (BEFTA) Programme. *Frontiers in Forests and Global Change*, *2*, 75.

552 Luskin, M.S. & Potts, M.D. (2011). Microclimate and habitat heterogeneity through the oil
553 palm lifecycle. *Basic and Applied Ecology*, *12*(6), 540-551.
554 Marsh, C.W. & Greer, A.G. (1992). Forest land-use in Sabah, Malaysia: an introduction to
555 Danum Valley. *Philosophical Transactions of the Royal Society of London. Series B:*
556 *Biological Sciences*, *335*(1275), 331-339.
557 Meijide, A., Badu, C.S., Moyano, F., Tiralla, N., Gunawan, D. & Knohl, A. (2018). Impact of
558 forest conversion to oil palm and rubber plantations on microclimate and the role of the
559 2015 ENSO event. *Agricultural and forest meteorology*, *252*, 208-219.
560 Mendoza, S.V., Harvey, C.A., Sáenz, J.C., Casanoves, F., Carvajal, J.P., Villalobos, J.G., ...
561 Sinclair, F.L. (2014). Consistency in bird use of tree cover across tropical agricultural
562 landscapes. *Ecological Applications*, *24*(1), 158-168.
563 Mitchell, S.L., Edwards, D.P., Bernard, H., Coomes, D., Jucker, T., Davies, Z.G. & Struebig,
564 M.J. (2018). Riparian reserves help protect forest bird communities in oil palm
565 dominated landscapes. *Journal of applied ecology*, *55*(6), 2744-2755.
566 Nagy, R.C., Porder, S., Neill, C., Brando, P., Quintino, R.M. & Nascimento, S.A.D. (2015).
567 Structure and composition of altered riparian forests in an agricultural Amazonian
568 landscape. *Ecological Applications*, *25*(6), 1725-1738.
569 Nichols, E.S. & Gardner, T.A. (2011). Dung beetles as a candidate study taxon in applied
570 biodiversity conservation research. *Ecology and evolution of dung beetles*, 267-291.
571 Oksanen, J., Blanchet, F.G., Kindt, R., Legendre, P., O'hara, R.B., Simpson, & Wagner, H.
572 (2010). Vegan: community ecology package. R package version 1.17-4. *URL*
573 http://CRAN.R-project.org/package=vegan.
574 QGIS Development Team (2020). QGIS Geographic Information System. Open Source
575 Geospatial Foundation Project. http://qgis.osgeo.org.
576 Schulze, C.H., Linsenmair, K.E. & Fiedler, K. (2001). Understorey versus canopy: patterns of
577 vertical stratification and diversity among Lepidoptera in a Bornean rain forest. *Plant*
578 *Ecology, 153*, 133–152.
579 Silvério, D.V., Brando, P.M., Macedo, M.N., Beck, P.S., Bustamante, M. & Coe, M.T. (2015).
580 Agricultural expansion dominates climate changes in southeastern Amazonia: the
581 overlooked non-GHG forcing. *Environmental Research Letters*, *10*(10), 104015.
582 Slade, E.M., Mann, D.J. & Lewis, O.T. (2011). Biodiversity and ecosystem function of tropical
583 forest dung beetles under contrasting logging regimes. *Biological Conservation*, *144*(1),
584 166-174.
585 Smith, J.M.B. (1977). Vegetation and microclimate of east-and west-facing slopes in the
586 grasslands of Mt Wilhelm, Papua New Guinea. *The Journal of Ecology*, *65*(1), 39-53.
587 Struebig, M.J., Turner, A., Giles, E., Lasmana, F., Tollington, S., Bernard, H. & Bell, D.,
588 (2013). Quantifying the biodiversity value of repeatedly logged rainforests: gradient
589 and comparative approaches from Borneo. *Advances in ecological research*, *48*, 183-
590 224.
591 Tabacchi, E., Lambs, L., Guilloy, H., Planty-Tabacchi, A.M., Muller, E. & Decamps, H.,
592 (2000). Impacts of riparian vegetation on hydrological processes. *Hydrological*
593 *processes*, *14*(16-17), 2959-2976.
594 R Development Core Team (2008). *R: A language and environment for statistical computing*.
595 Vienna, Austria: R Foundation for Statistical Computing. http://www.R-
596 project.org.ISBN3-900051-07-0
597 Travis, J.M.J. (2003). Climate change and habitat destruction: a deadly anthropogenic cocktail.
598 *Proceedings of the Royal Society of London. Series B: Biological Sciences*, *270*(1514),
599 467-473.
600 Walsh, R.P.D. & Newbery, D.M. (1999). The ecoclimatology of Danum, Sabah, in the context
601 of the world's rainforest regions, with particular reference to dry periods and their

impact. *Philosophical Transactions of the Royal Society of London. Series B: Biological Sciences*, *354*(1391), 1869-1883.
Williams, A.P., Allen, C.D., Macalady, A.K., Griffin, D., Woodhouse, C.A., Meko, D.M., ... Dean, J.S. (2013). Temperature as a potent driver of regional forest drought stress and tree mortality. *Nature climate change*, *3*(3), 292-297.
Williams-Linera, G. (1990). Vegetation structure and environmental conditions of forest edges in Panama. *The Journal of Ecology*, 356-373.
Zellweger, F., De Frenne, P., Lenoir, J., Rocchini, D. & Coomes, D. (2019). Advances in microclimate ecology arising from remote sensing. *Trends in ecology & evolution*, *34*(4), 327-341.
Zimbres, B., Peres, C.A. & Machado, R.B. (2017). Terrestrial mammal responses to habitat structure and quality of remnant riparian forests in an Amazonian cattle-ranching landscape. *Biological Conservation*, *206*, 283-292.

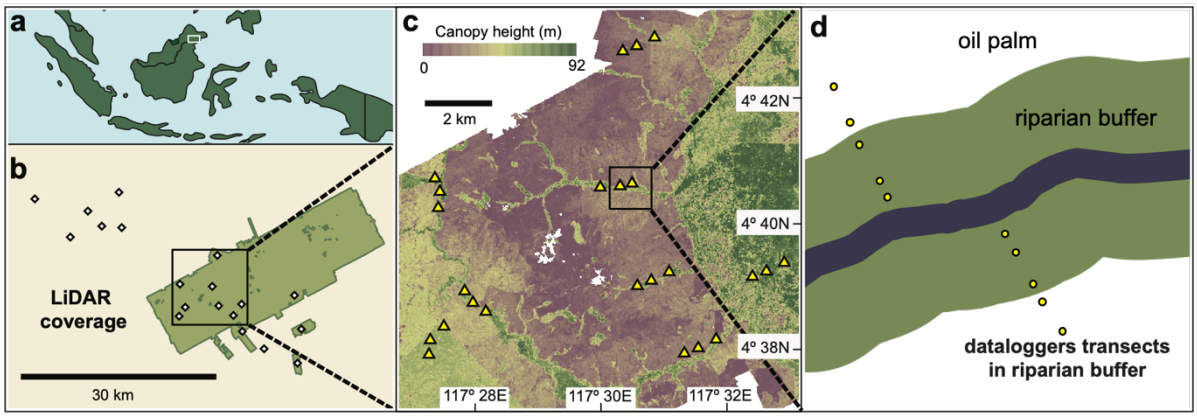

Figure 1 - Study location and design. (a) Map of SouthEast Asia with panel B denoted by a white rectangle. (b) Study landscape with the green silhouette denoting the airborne LiDAR-scan area, and points denoting the 20 study rivers. A black square denotes the area shown in panel c. (c) LiDAR-derived canopy height model of part of our study landscape. Yellow triangles denote sampling transects (n=60). (d) Sampling design for a riparian buffer transect. Yellow circles denote datalogger points. Positions of dataloggers are (from river outwards) 5 m from the river, 15 m from the river, ~5 m from the buffer-oil-palm edge, 5 m into oil palm and 25 m into oil palm. The blue line denotes the river.

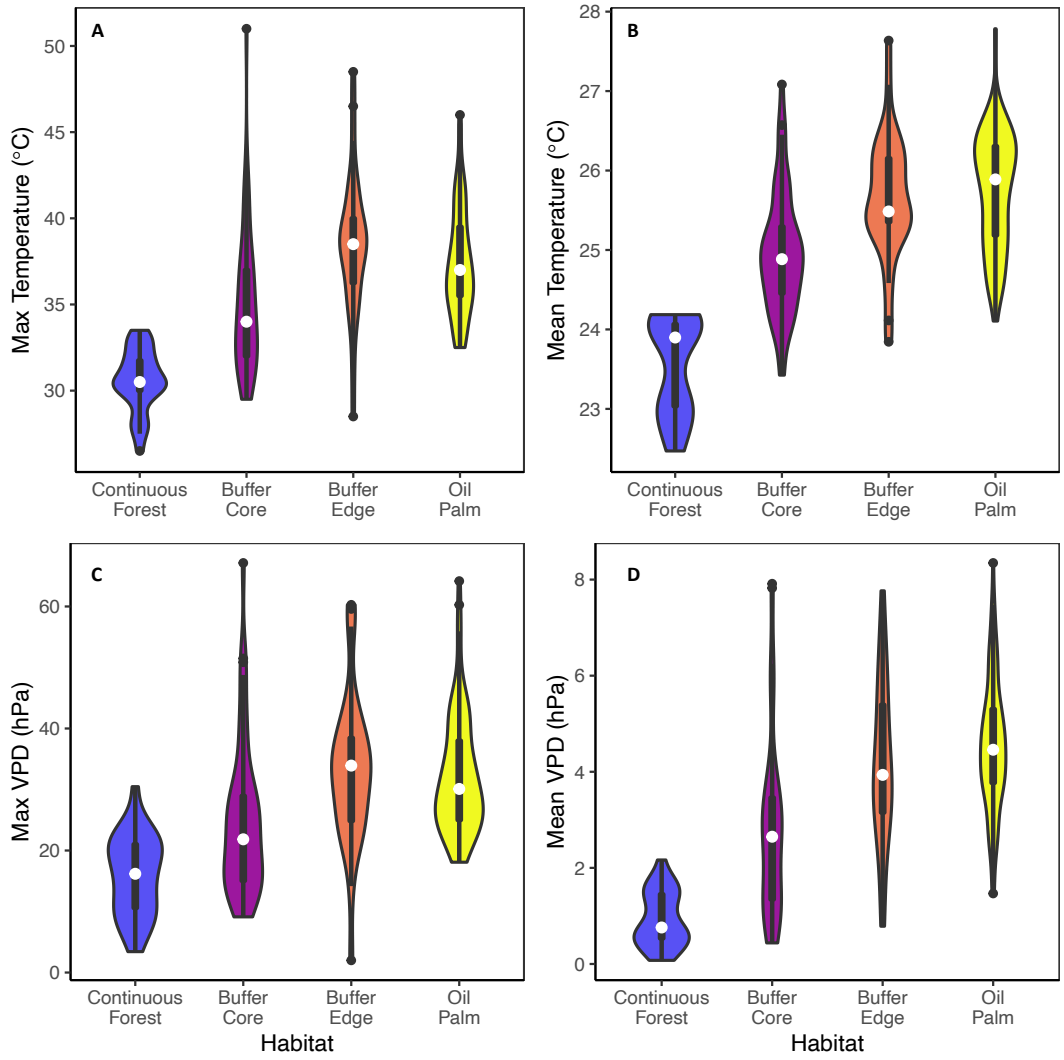

627
628 ***Figure 2*** **-** Violin plots of daily maximum (T_{max}, panel A), and mean (T_{mean}, panel B)
629 temperature, and daily maximum (VPD_{max}, panel C) and mean (VPD_{mean}, panel D) vapour
630 pressure deficit across habitat types. White circles are median values, the boxes are between
631 the hinge values (25th and 75th percentiles), and the whiskers are the hinge values + or -
632 interquartile range * 1.5. Data that lie outside of the box and whisker plots are denoted by dark
633 circles.

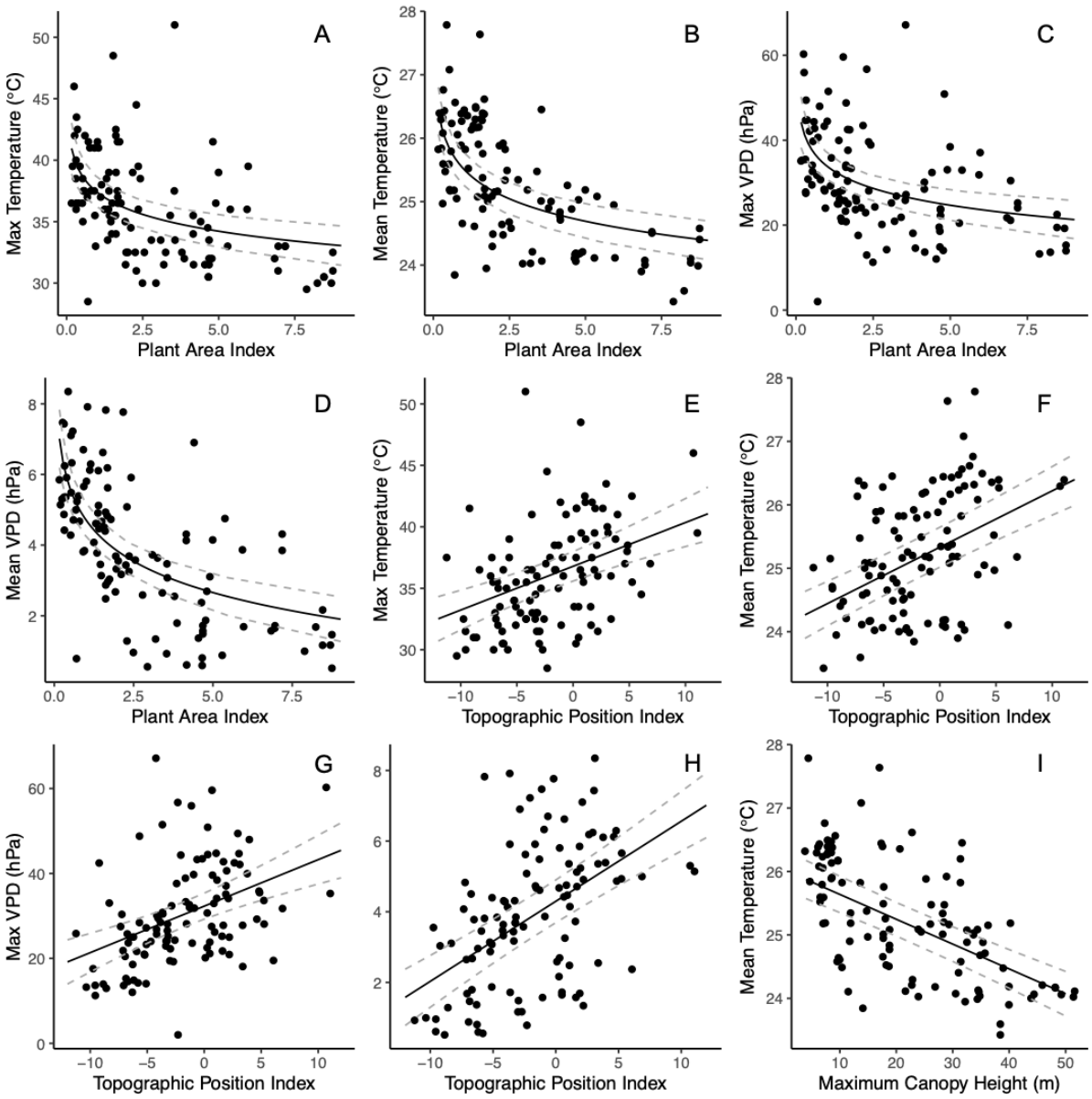

Figure 3 - Scatter plots showing the effect of Plant Area Index (PAI) (A-D) and Topographic Position Index (TPI) (E-H) on T_{max} , T_{mean}, VPD_{max} and VPD_{mean}, and the effect of maximum canopy height (H_{max}) on T_{mean} (I). Solid lines are estimated effects from linear mixed effects models where TPI or PAI were the only fixed effect, with dashed lines denoting 95% confidence intervals. PAI is back-transformed from data used in analyses. A positive TPI is associated with ridges and a negative TPI with depressions.

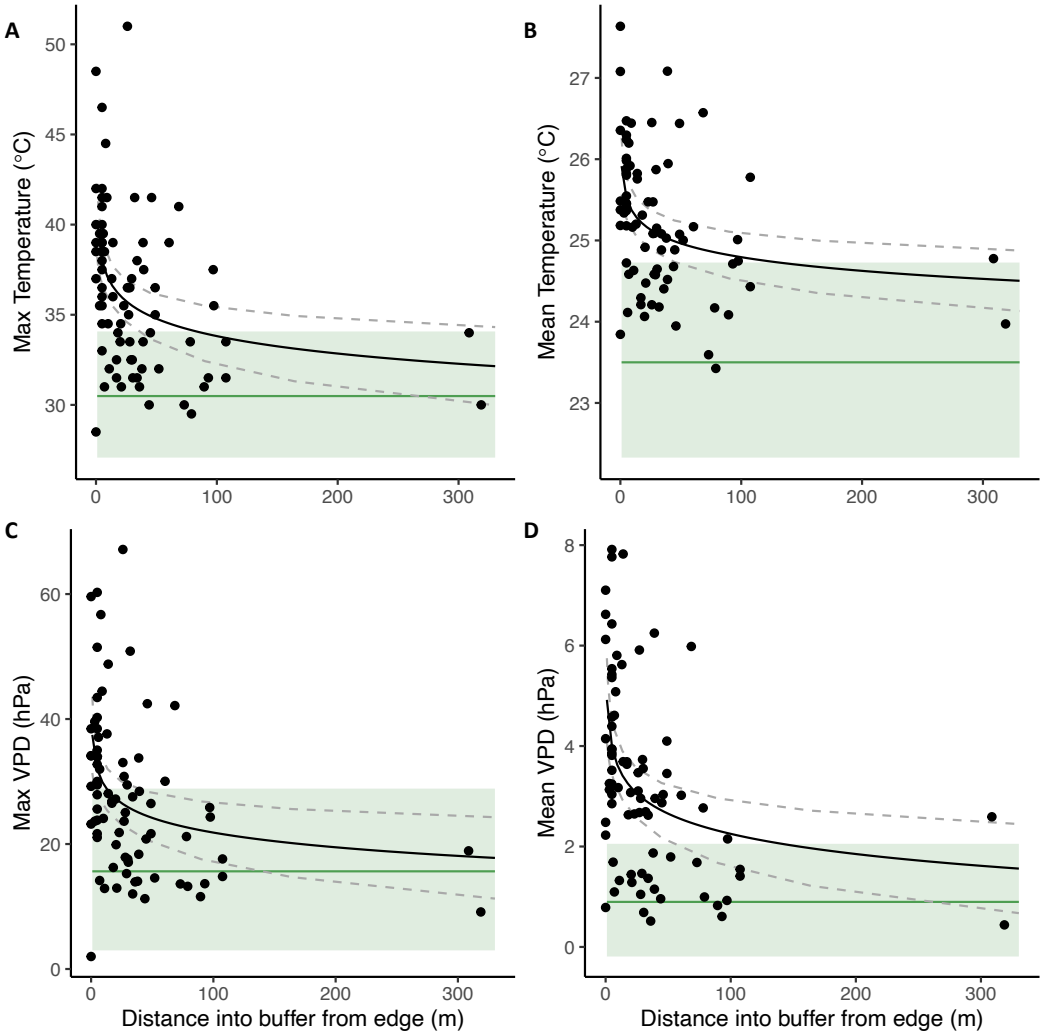

Figure 4 - Scatter plots showing the effect of distance into the buffer from the buffer-oil-palm edge on T_{max}, T_{mean}, VPD_{max} and VPD_{mean} (panels A, B C and D, respectively). Black lines are back-transformed from log-transformed distance predicted from linear mixed effects models, with dashed lines denoting 95% confidence intervals. Solid green lines denote mean microclimatic values for continuous riparian forest, with 95% confidence intervals shown in green bands.

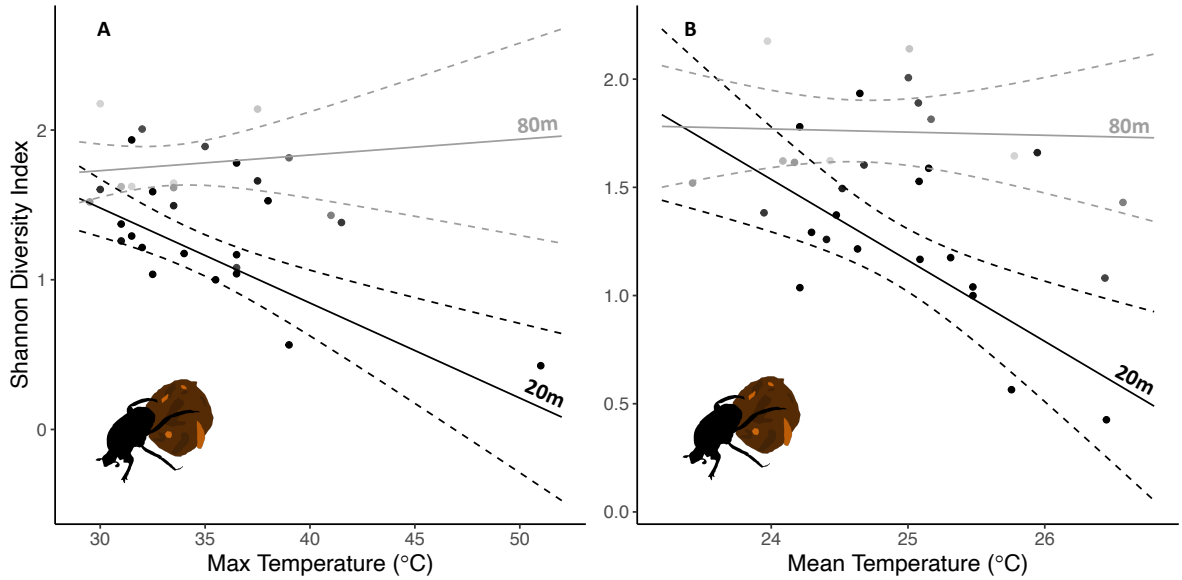

650
651
652 ***Figure 5 -*** Visualisations of the interaction between the effects of (A) T_{max} and (B) T_{mean}, and
653 distance from edge on dung beetle diversity. Solid lines give the effect of temperature on
654 diversity, given two set distances (20m and 80m) from the edge of the buffer, as predicted using
655 estimates from linear models (see Table 3), with dashed lines denoting 95% confidence
656 intervals. Grey-scaling on points and lines gives the magnitude of distance from buffer edge
657 (grey > black).

658 **Table 1** - Effect sizes and standard errors of habitat type on T_{max}, T_{mean}, VPD_{max} and VPD_{mean}
659 using linear mixed-effects models.
660

response variables	Continuous Forest		Riparian Buffer		Buffer Edge		Oil Palm	
	estimate	se	estimate	se	estimate	se	estimate	se
T_{max} (°C)	30.57	0.34	35.05	0.58	38.45	0.73	37.37	0.33
T_{mean} (°C)	23.53	0.12	24.96	0.11	25.66	0.14	25.75	0.08
VPD_{max} (hPa)	15.92	1.27	24.76	1.71	33.08	2.20	32.20	1.01
VPD_{mean} (hPa)	0.93	0.11	2.71	0.25	4.15	0.31	4.53	0.14

661

Table 2 - Weighted-proportions of the retention of each fixed effect across best-fitting models for T_{max} , T_{mean}, VPD_{max} and VPD_{mean}. AIC weights were generated for all models, before models were subsetted to include only those that cumulatively made up 0.95 of the total weight. AIC w. prop. is the proportion of the 0.95 cumulative weight constituted by models containing the fixed effect of interest. Values given in bold fell above an arbitrary threshold value of 0.5. Effect sizes of models with only a single explanatory variable are given, with the exception of habitat, as it is a categorical variable (see Table 1). PAI, TPI and H_{max} are abbreviations for Plant Area Index, Topographic Position Index and maximum canopy height, respectively. A positive TPI is associated with ridges and a negative TPI with depressions.

	T_{max}		**T_{mean}**		**VPD_{max}**		**VPD_{mean}**	
fixed effects	*AIC w. prop.*	*effect*	*AIC w. prop.*	*effect*	*AIC w. prop.*	*effect*	*AIC w. prop.*	*effect*
PAI	**0.930**	**-1.980**	**1.000**	**-0.512**	**0.950**	**-5.726**	**1.000**	**-1.279**
H_{max}	0.362	-0.134	**0.642**	**-0.039**	0.324	-0.384	0.410	-0.095
TPI	**0.899**	**0.357**	**1.000**	**0.089**	**0.924**	**1.096**	**0.955**	**0.226**
elevation	**0.692**	**-0.0011**	**1.000**	**-0.0027**	0.275	-0.0010	0.273	0.0048
aspect	0.366	0.182	**0.978**	**0.224**	0.304	1.640	**0.559**	**0.427**
slope	0.310	-3.024	0.463	-1.58	0.273	-9.229	0.258	-4.041
aspect : H_{max}	0.090	0.220	0.176	0.072	0.047	0.006	0.065	0.011
habitat type	**1.000**	**-**	**1.000**	**-**	0.467	-	**0.861**	**-**

673 ***Table 3*** **-** AIC weights of all models of Shannon Diversity for each microclimatic variable
674 (T_{max}, T_{mean}, VPD_{max} and VPD_{mean}), where 'interaction' denotes models containing the
675 interaction term between buffer width and microclimate, 'additive' denotes a model containing
676 microclimate and buffer width, 'buffer width' and 'microclimate' denote models containing
677 only that term, and 'null' is the null model. Values given in bold make up the best-fitting
678 models, as calculated by a cumulative ranked weight > 0.95.
679

models	$\boldsymbol{T_{max}}$	$\boldsymbol{T_{mean}}$	$\boldsymbol{VPD_{max}}$	$\boldsymbol{VPD_{mean}}$
interaction	**0.959**	**0.914**	**0.723**	**0.354**
additive	0.038	**0.068**	**0.271**	**0.573**
buffer width	0.003	0.018	0.005	**0.068**
microclimate	<0.001	<0.001	<0.001	0.005
null	<0.001	<0.001	<0.001	0.001

680

Table 4 - Outputs of best-fitting linear models predicting the Shannon diversity of dung beetles (H') sampled in riparian buffers. In the model column '~' means 'as a function of' and '*' means the two terms individually and the interaction between the two are included.

model	term	estimate	SE
H' ~ T_{max} * distance from edge	intercept	7.645	2.215
	T_{max}	-0.223	0.067
	distance from edge	-1.422	0.607
	T_{max} : distance from edge	0.053	0.018
H' ~ T_{max} + distance from edge	intercept	1.355	0.532
	T_{max}	-0.032	0.012
	distance from edge	0.333	0.073
H' ~ T_{mean} * distance from edge	intercept	28.66	9.446
	T_{mean}	-1.151	0.382
	distance from edge	-6.057	2.407
	T_{mean} : distance from edge	0.259	0.098
H' ~ T_{mean} + distance from edge	intercept	3.939	1.821
	T_{mean}	-0.150	0.070
	distance from edge	0.338	0.077
H' ~ VPD_{max} * distance from edge	intercept	1.398	0.485
	VPD_{max}	-0.053	0.021

	distance from edge	0.903	0.129
	VPD_{max} : distance from edge	0.012	0.006
$H' \sim VPD_{max}$ + distance from edge	intercept	0.668	0.315
	VPD_{max}	-0.013	0.004
	distance from edge	0.300	0.072
$H' \sim VPD_{mean}$ * distance from edge	intercept	0.869	0.434
	VPD_{mean}	-0.216	0.142
	distance from edge	0.214	0.109
	VPD_{mean} : distance from edge	0.039	0.041
$H' \sim VPD_{mean}$ + distance from edge	intercept	0.617	0.345
	VPD_{mean}	-0.084	0.033
	distance from edge	0.285	0.080
$H' \sim$ distance from edge	intercept	0.104	0.302
	distance from edge	0.365	0.080

685

686 ***Table 5 -*** Microclimate buffering with distance inward from buffer edge, as estimated from
687 linear mixed-effects models. Values given reflect the difference relative to the microclimate in
688 oil palm (Table 1).

response variables	**5 m**	**20 m**	**40 m**	**80 m**	**300 m**
T_{max} (°C)	0.36	-1.58	-2.55	-3.51	-5.36
T_{mean} (°C)	-0.23	-0.57	-0.73	-0.90	-1.23
VPD_{max} (hPa)	-0.80	-5.50	-7.85	-10.21	-14.69
VPD_{mean} (hPa)	-0.57	-1.37	-1.77	-2.17	-2.94

689